

FIRST AND SECOND LAW EVALUATION OF COMBINED BRAYTON-ORGANIC RANKINE POWER CYCLE

Önder Kaşka¹, Onur Bor², Nehir Tokgöz^{3*} Muhammed Murat Aksoy⁴

ABSTRACT

In the present work, we have conducted thermodynamic analysis of an organic Rankine cycle (ORC) using waste heat from intercooler and regenerator in Brayton cycle with intercooling, reheating, and regeneration (BCIRR). First of all, the first law analysis is used in this combined cycle. Several outputs are revealed in this study such as the cycle efficiencies in Brayton cycle which is dependent on turbine inlet temperature, intercooler pressure ratios, and pinch point temperature difference. For all cycles, produced net power is increased because of increasing turbine inlet temperature. Since heat input to the cycles takes place at high temperatures, the produced net power is increased because of increasing turbine inlet temperature for all cycles. The thermal efficiency of combined cycle is higher about 11.7% than thermal efficiency of Brayton cycle alone. Moreover, the net power produced by ORC has contributed nearly 28650 kW. The percentage losses of exergy for pump, turbine, condenser, preheater I, preheater II, and evaporator are 0.33%, 33%, 22%, 23%, 6%, and 16% respectively. The differences of pinch point temperature on ORC net power and efficiencies of ORC are investigated. In addition, exergy efficiencies of components with respect to intercooling pressure ratio and evaporator effectiveness is presented. Exergy destructions are calculated for all the components in ORC.

Keywords: *Brayton Cycle, Organic Rankine Cycle, Bottoming Cycle, Pinch Point Temperature, Waste Heat, Energy and Exergy Analysis*

INTRODUCTION

Thermal energy systems as well as corresponding all parts have been challenged to improve overall efficiency due to lack of conventional fuels, reduce climate change and so on for recent years. The crucial part of this issue is to conduct the development case for both thermodynamic and economic perspectives. Gas turbine industry would be illustrated as a thorough example since its development process has stimulated several related fields, e.g., blade cooling, aerodynamics, material choosing, etc. in order to accomplish thermodynamic and economic goals. In addition, it would be noted that numerous researchers have worked in different subjects such as working fluid selection, bottoming cycle, waste heat recovery areas to increase both first and second law thermodynamic efficiencies. He et al. investigated 22 working fluids of subcritical organic Rankine cycle (ORC) for waste heat recovery in order to find out optimum temperature for evaporation. Their theoretical results are compared with numerical simulations and results in the literature. They have determined four criteria such as the maximum net power output, suitable working pressure, total heat transfer capacity and expander size parameter to examine the working fluids [1]. Carcasci et al. selected toluene, benzene, cyclohexane and cyclopentane as the working fluids in order to analyze their ORC system from thermodynamic perspective. Their results showed that the aforementioned fluids give best results without the super heater except cyclopentane. They have demonstrated that at the end of the study cyclohexane and cyclopentane provide the optimum working pressure [2]. An integrated gas turbine-modular helium reactor cycle examined by Yaria and Mahmoudi. They calculated the first and second law efficiency for each component, and it has been optimized by using EES software. The results presented at this study reveal that increasing the temperature of the turbine inlet is directly related with the first and second law efficiencies and power generation. They, finally, revealed the first law efficiency of their current system is increased up to 2.93% [3]. Clemente et al. were to design a bottoming cycle for the regenerative gas turbine by working on different expanders for organic Rankine cycle (ORC). They have optimized six different working fluids to maximize delivered power in order to use them either axial or radial turbines. As a result of their work, it is noted that using the refrigerants such as R245fa, isopentane and isobutene give rise to more reasonable results rather than siloxane at their ORC system [4]. Roy and Mishra conducted a thermodynamic analysis of the regenerative organic Rankine cycle (ORC) for specific conditions. Their aim is to choose relatively a better working fluid for system efficiency, turbine outflow, irreversibility and second law efficiency for different operating conditions. It is found out that R-123 is preferable as a working fluid compared to R-134 in order to

This paper was recommended for publication in revised form by Regional Editor Erman Aslan

^{1,2}Department of Mechanical Engineering, Osmaniye Korkut Ata University, Osmaniye, Turkey

³Department of Energy Systems Engineering, Osmaniye Korkut Ata University, Osmaniye, Turkey

⁴Department of Mechanical Engineering, Rice University, Houston, United States

*E-mail address: nehirtokgoz@osmaniye.edu.tr

Orcid id: 0000-0002-7284-2093, 0000-0001-9767-8202, 0000-0001-9264-9971, 0000-0001-7594-9462

Manuscript Received 03 September 2018, Accepted 22 January 2019

convert the heat, which is low-graded, into the useful power [5]. Wang et al. performed a simulated annealing algorithm in order to analyze and optimize the working fluid and its parameters for the ORC cycle. Temperatures effects of waste heat as well as its economic consequences were investigated for several optimum cases [6]. Sun and Li comprehensively investigated a heat recovery power plant of the ORC using R134a as a working fluid. They developed mathematical models on system components (such as expander, evaporator, condenser, pump) to examine the performance of the plant. Also, they have offered an optimum algorithm to ascertain the controlled variables [7]. Wei et al. performed thermodynamic analysis for HFC-245fa as well as optimization of the ORC. In general, augmentation of the net power and efficiency obtained from the cycle are induced from the increase of the exhaust heat. Finally, they have had three main conclusions to improve thermal performance of the system, and they are concisely using the exhaust heat at the ultimate level, low temperature level at condenser outlet, and low ambient temperature [8]. Ahmadi et al. conducted an integrated ORC for trigeneration. They have indicated that combustion chamber and heat exchanger are the principal sections of most of the exergy destruction. They have proved that compressor pressure ratio, turbine inlet, and outlet temperatures have significantly influenced on the system efficiency. Furthermore, CO₂ emissions of the trigeneration cycle are at the lower level compared to micro gas turbines and combined heat and power (CHP) cycles [9]. Chacartegui et al. studied a bottoming organic Rankine cycle, which is designed for low temperature, for several types of combined heat and power plants. They have the intention to reveal alternative cycles for specific gas turbines such as recuperative gas turbines with low exhaust temperature. For this study, they have used six different organic working fluids in order to show the differences among them [10]. The non-regenerative organic Rankine cycle (ORC) analysis was performed by Roy et al. using different working fluids superheated at constant pressure. In order to analyze and optimize the necessary outputs for the efficiency of the thermal system such as second law evaluation, work output, availability ratio, etc. a Fortran code was written by changing heat source temperature as the input parameter [11]. For the waste heat recovery, Tau et al. revealed the effects of working fluids on ORC. For this reason, they have used various working fluids to characterize the effects on the thermal efficiency as well as the total heat recovery efficiency [12]. Meinel et al. have investigated the first and second law analyzes of ORC applications taking into account the acid gas condensation temperatures. As a result of their work, it can be indicated that dry fluids would be more efficient in the recuperator cycle [13]. Cao et al. have worked on an ORC as a dip cycle for the use of waste heat from gas turbines. The results show that the ORC type together with the input inlet pressure increase the net power and thermal efficiency of the ORC and achieve optimal values at a given pressure based on the optimum criterion. For the combined cycle, toluene was decided rather as appropriate a working fluid than the other fluids [14]. Evelyoy et al. have presented solid oxide fuel cell-gas turbine-ORC combined cycle both thermodynamic and economic perspectives. They have used six different working fluids such as toluene, benzene, cyclohexane, cyclopentane, R123 and R245fa in this cycle and they have performed energy and exergy analysis. Using toluene as working fluid, they have calculated 64% and 62% increases in energy and exergy efficiencies, respectively, of solid oxide fuel cell (SOFC) system and bottoming organic Rankine cycle systems [15]. Kaska has revealed energy and exergy analyses of an ORC for power generation from waste heat recovery. He concluded that the evaporation pressure plays a crucial role on both energy and exergy efficiency. Therefore, pinch point analysis was revealed to understand the effects of heat exchange process in the evaporator, and also the effects on the net power production are shown from the results of pinch point analysis [16]. Camporeale et al. have made energy analysis of externally fired gas turbine and organic Rankine combined cycle, and they conducted various bottoming cycles to bring about the effects of evaporation pressure and superheating temperature of the system. They have used various organic fluids such as siloxanes and toluene to examine effects on the plant performance [17]. Maraver et al. have revealed the optimization of an organic Rankine cycle for power generation by combining different heat sources for cogeneration. The impression of the study would be that how combining different working fluids and heat sources can be considered as the essentials to design and optimize the ORC systems [18]. Li et al. have conducted the effects of pinch point temperature difference on performance of organic Rankine cycle. It is shown that net power output would not be maximized for different organic working fluids because of the corrosion at low temperature levels. Also, they have stated the raise of pinch point temperature difference at the evaporator would cause fluctuation of the total heat transfer area, yet the net power output per total area exhibits conversely proportional sign. It is finally noted that isentropic fluids would rather be preferable than dry working fluids for the performance case [19]. Tian et al. have revealed optimization for organic Rankine Cycle in exhaust heat recovery for an internal combustion engine. They techno-economically analyzed the results for twenty different working fluids. They calculated the ORC thermal efficiency, expansion ratio, net power output per unit mass flow rate of hot exhaust,

net power output ratio of total heat transfer area, and electricity generation cost for each selected working fluid [20]. Karellas et al. have examined energy and exergy analysis of water-steam and organic Rankine cycle for waste heat recovery. For temperature of exhaust gases higher than 310°C, the efficiency of water-steam cycle would be better than ORC. The waste heat recovery installations in the cement industry indicate that electricity consumption has deteriorated significantly and the payback of this investment is up to 5 years [21]. Hajabdollahi et al. have designed an optimum organic Rankine Cycle for diesel engine waste heat recovery. They selected various refrigerants such as R123, R134a, R245fa and R22, and from both economic and thermodynamic perspectives, R123 is determined as the best working fluid compared to others [22]. Astolfi et al. scrutinized the ORC for low temperature geothermal sources. In order to obtain maximum system efficiency for supercritical cycles, they found out that critical temperature of the working fluid must be lower than the geothermal source temperature [23]. Carcasci et al. showed thermodynamic analysis of organic Rankine cycle combined with gas turbine. They have compared various working fluids such as toluene, benzene, cyclopentane and cyclohexane for the best choice. Sensitivity analysis is performed to explore the uncertainty in the inputs of ORC system, i.e., changing the pressure for various temperature inlets [2]. Guo et al. have analyzed an organic Rankine cycle from the location of heat transfer pinch point in evaporator. If heat source is low, supercritical ORC would create superior efficiency with regards to both thermal and exergy performance. For subcritical ORC, the contrary is valid [24]. Tuo has used various working fluids to analyze an organic Rankine cycle for waste heat recovery from a solid oxide fuel cell - gas turbine hybrid power cycle. It is shown that how working fluid would be chosen for various working parameters. Also, it is revealed from the results that the temperatures of turbine inlet, exhaust gas, and fluid's critical point have directly related with the efficiency of the ORC system [25]. For further review studies, readers are recommended to refer to the following articles [26-29]. This paper reveals a comprehensive thermodynamic analysis and optimization of combined Brayton and Organic Rankine Cycle (ORC). Thermo-dynamic analysis of combine intercooler and exhaust of regenerator as heat source for ORC comes to the fore. Analyzing the effects of various design parameters on the cycle performance, a parametric study was conducted. By using Engineering Equation Solver (EES) [30], essential parameters are being calculated and they would be counted as intercooling pressure ratio, turbine inlet temperature, evaporator outlet temperature and pinch point temperature difference on the first law efficiency.

SYSTEM DESCRIPTION

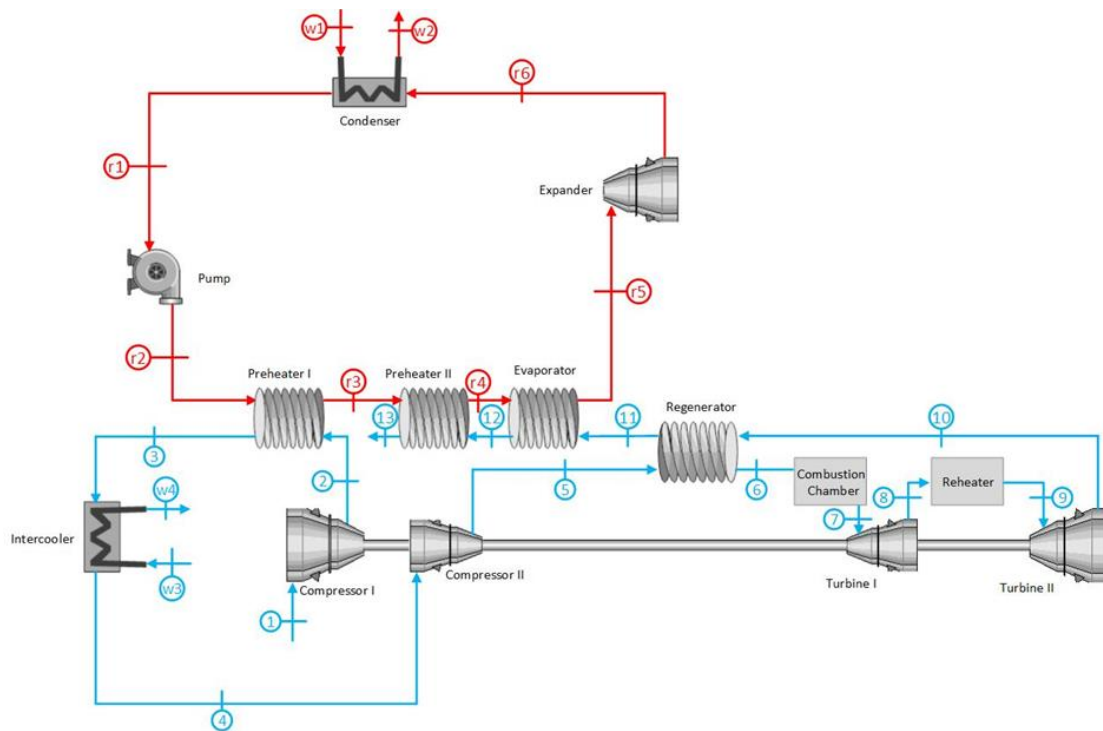


Figure 1. The combined organic rankine-brayton cycle model

In the present study, energy analysis [31] of the combined organic Rankine-Brayton cycle is scrutinized, and toluene is the working fluid. The schematic representation of the combined organic Rankine-Brayton cycle can be seen in Figure 1.

In the Brayton cycle with intercooling, reheating and regeneration, ambient air (P_1) is compressed isentropically in the compressor at the first stage and is cooled to state 4 at constant pressure ($P_2 = P_4$). It enters to the second stage compressor and is compressed isentropically to the highest-pressure value (P_5). It is heated by entering to the regenerator at constant pressure (T_6). Heated air at combustion chamber goes to the high-pressure turbine. After the re-heater, temperatures at the inlet of the turbine 1 and turbine 2 are equal to each other ($T_7 = T_9$). Finally, air is continued to cool to the stage 13 at constant pressure for the Brayton cycle. Organic Rankine cycle which is used as an intercooler and a heat recovery unit consists of pump, preheater, evaporator, turbine and condenser. Working fluid enters the pump as a saturated liquid and is compressed to the state r2 (P_{r2}) from state r1 (P_{r1}). Working fluid which leaves the pump enters to the preheater and is heated to the state r4 (saturated liquid temperature) at constant pressure. After the evaporator, it leaves as a saturated vapor. In ORC turbine, it is expanded to state r6 (P_{r6}) from state r5 (P_{r5}) and it is cooled to the state r1 (T_{r1}) from state r6 (T_{r6}) at constant pressure. Assumption values and the properties at various states for ORC-Brayton combined cycle are given in Table 1 and Table 2.

Table 1. Assumption values for ORC-brayton combined cycle

Item	Value
Inlet temperature of first stage compressor, (T_1) (°C)	25 [32]
Inlet pressure of first stage compressor, (p_1) (bar)	1
Brayton compressor isentropic efficiency, (η_{c1}, η_{c2}) (%)	75[33]
Brayton turbine isentropic efficiency, (η_{T1}, η_{T2}) (%)	80[33]
Effectiveness of regenerator, ($\eta_{reg.}$) (%)	80[33]
ORC pump isentropic efficiency, (η_p) (%)	80[34]
ORC expander isentropic efficiency, (η_T) (%)	80[34]
Preheater I effectiveness, (%)	85[34]
Preheater II effectiveness, (%)	85[34]
Evaporator effectiveness, (%)	85[34]
Pinch point temperature difference in the evaporator, (ΔT_{pp}) (°C)	12.5

Table 2. The properties at various states for ORC-Brayton combined cycle

State no.	Fluid	Phase	Temperature, T (°C)	Pressure, P (bar)	Enthalpy, h (kJ/kg)	Entropy, s (kJ/kg-K)
1	Air	-	25	1	298.4	6.862
2	Air	-	170.7	3	445.6	6.949
3	Air	-	110.8	3	384.7	6.801
4	Air	-	25	3	297.9	6.546
5	Air	-	170.8	9	445.2	6.632
6	Air	-	720.9	9	1040	7.498
7	Air	-	1100	9	1484	7.875
8	Air	-	842.4	3	1180	7.946
9	Air	-	1100	3	1484	8.191
10	Air	-	842.4	1	1179	8.261
11	Air	-	305.1	1	584.6	7.538
12	Air	-	234.3	1	511	7.402
13	Air	-	190.1	1	465.6	7.309
r1	Toluene	Sat. liquid	35	0.06249	-141	-0.4079
r2	Toluene	Comp. liquid	35.43	10.81	-139.5	-0.4069
r3	Toluene	Comp. liquid	150.2	10.81	82.92	0.2023
r4	Toluene	Sat. liquid	221.8	10.81	248.6	0.5632
r5	Toluene	Sat. vapor	221.8	10.81	516.9	1.106
r6	Toluene	Sup. vapor	112.1	0.06249	367.6	1.206

Organic Rankine Cycle Model

Organic Rankine cycle (ORC) is used as the intercooler of the system, and the thermal efficiency of ORC and net produced power are calculated in this section. It is assumed that the fluid enters to the evaporator as saturated liquid. The pressure at the evaporator inlet is taken as equivalent to the pressure at the evaporator outlet ($P_{r4}=P_{r5}$). Also, the fluid at the inlet of the pump is considered as saturated liquid and the condenser temperature is taken 35°C. T-s diagram of the organic Rankine cycle shown in Figure 2.

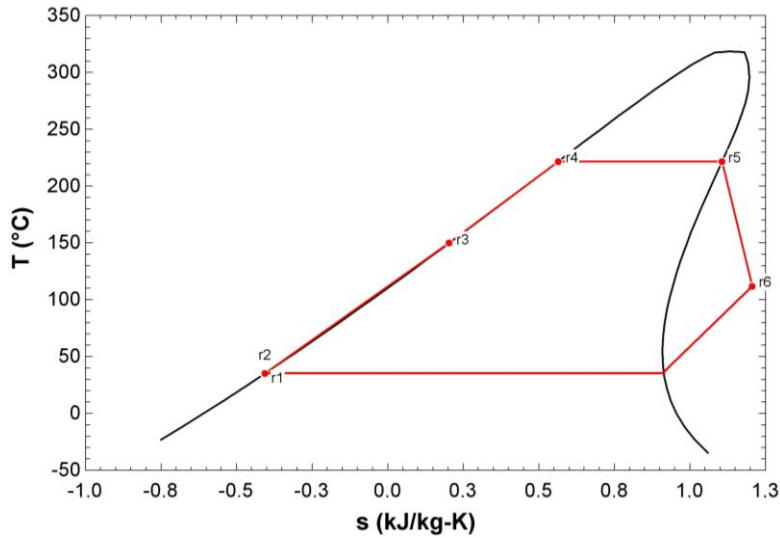


Figure 2. T-s diagram of organic rankine cycle

The net power produced by ORC is shown as

$$\dot{W}_{net,ORC} = \dot{W}_{expander,ORC} - \dot{W}_{pump,ORC} \quad (1)$$

The thermal efficiency of ORC is evaluated by using Eq. 2

$$\eta_{ORC} = \frac{\dot{W}_{net,ORC}}{\dot{Q}_{preheater,I} + \dot{Q}_{preheater,II} + \dot{Q}_{evaporator}} \quad (2)$$

Mass, energy and exergy equations for organic Rankine cycle are given in Table 3.

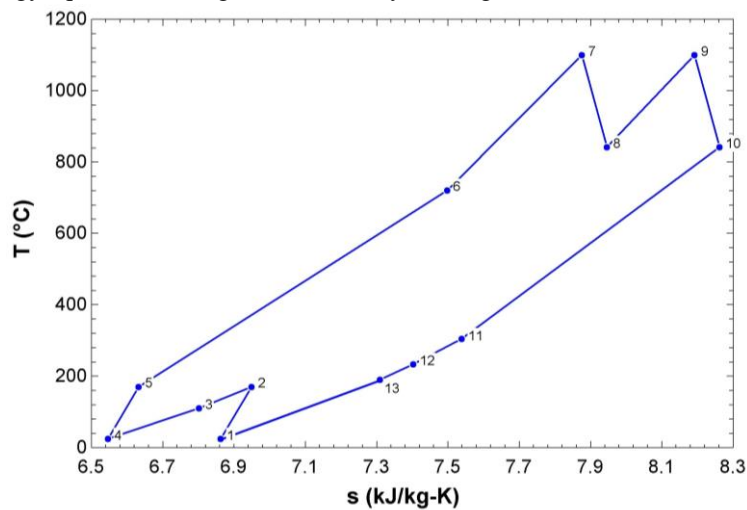
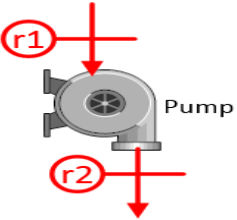
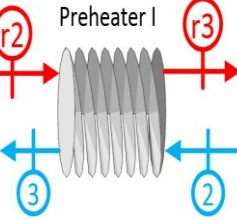
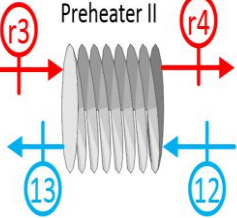
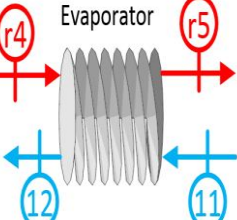
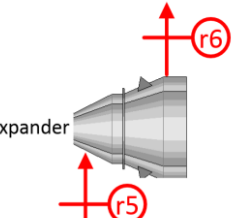
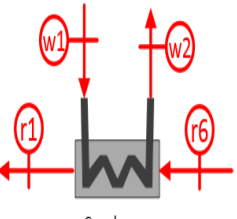


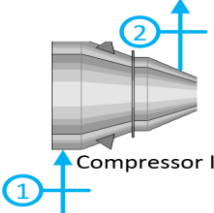
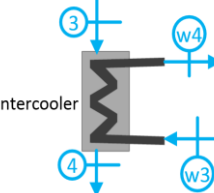
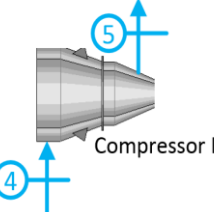
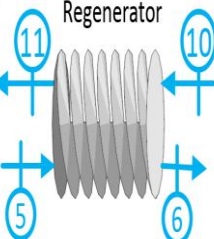
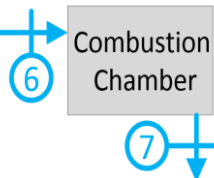
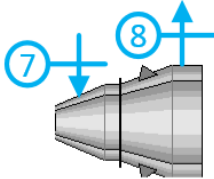
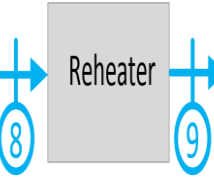
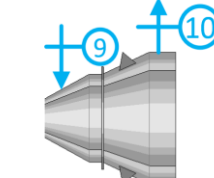
Figure 3. T-s diagram of Brayton cycle

Table 3. Mass, energy and exergy relations for the components of organic Rankine cycle.

Cycle components	Mass, energy, and exergy equations
	$\dot{m}_{r1} = \dot{m}_{r2}$ $\eta_{pump} = \frac{h_{r2,s} - h_{r1}}{h_{r2} - h_{r1}}$ $\dot{W}_{pump} = \dot{m}_r (h_{r2} - h_{r1})$ $(\psi_{r1} + \dot{W}_{pump}) - \psi_{r2} - \dot{i}_{pump} = 0$ $\eta_{II,pump} = 1 - \left(\frac{\dot{i}_{pump}}{\dot{W}_{pump}} \right)$
	$\dot{m}_{r2} = \dot{m}_{r3}, \dot{m}_2 = \dot{m}_3$ $\dot{Q}_{preheater,I} = \dot{m}_r (h_{r3} - h_{r2})$ $\dot{Q}_{preheater,I} = \dot{m}_{air} (h_2 - h_3)$ $(\psi_2 + \psi_{r2}) - (\psi_3 + \psi_{r3}) - \dot{i}_{preheater,I} = 0$ $\eta_{II,preheater,I} = 1 - \left[\frac{\dot{i}_{preheater,I}}{(\psi_2 - \psi_3)} \right]$
	$\dot{m}_{r3} = \dot{m}_{r4}, \dot{m}_{12} = \dot{m}_{13}$ $\dot{Q}_{preheater,II} = \dot{m}_r (h_{r4} - h_{r3})$ $\dot{Q}_{preheater,II} = \dot{m}_{air} (h_{12} - h_{13})$ $(\psi_{12} + \psi_{r3}) - (\psi_{13} + \psi_{r4}) - \dot{i}_{preheater,II} = 0$ $\eta_{II,preheater,II} = 1 - \left[\frac{\dot{i}_{preheater,II}}{(\psi_{12} - \psi_{13})} \right]$
	$\dot{m}_{r4} = \dot{m}_{r5}, \dot{m}_{11} = \dot{m}_{12}$ $\dot{Q}_{evaporator} = \dot{m}_r (h_{r5} - h_{r4})$ $\dot{Q}_{evaporator} = \dot{m}_{air} (h_{11} - h_{12})$ $(\psi_{11} + \psi_{r4}) - (\psi_{12} + \psi_{r5}) - \dot{i}_{evaporator} = 0$ $\eta_{II,evaporator} = 1 - \left[\frac{\dot{i}_{evaporator}}{(\psi_{11} - \psi_{12})} \right]$
	$\dot{m}_{r5} = \dot{m}_{r6}$ $\eta_T = \frac{h_{r5} - h_{r6}}{h_{r5} - h_{r6,s}}$ $\dot{W}_{expander} = \dot{m}_r (h_{r5} - h_{r6})$ $\psi_{r5} - (\dot{W}_{expander} + \psi_{r6}) - \dot{i}_{expander} = 0$ $\eta_{II,expander} = 1 - \left[\frac{\dot{i}_{expander}}{(\psi_{r5} - \psi_{r6})} \right]$
	$\dot{m}_{r6} = \dot{m}_{r1}$ $\dot{m}_{w1} = \dot{m}_{w2}$ $\dot{Q}_{condenser} = \dot{m}_{w1} (h_{w2} - h_{w1})$ $\dot{Q}_{condenser} = \dot{m}_r (h_{r6} - h_{r1})$ $(\psi_{w1} + \psi_{r6}) - (\psi_{w2} + \psi_{r1}) - \dot{i}_{condenser} = 0$ $\eta_{II,condenser} = 1 - \left(\frac{\dot{i}_{condenser}}{\psi_{r6} - \psi_{r1}} \right)$

Mass, energy, and exergy equations for Brayton cycle are given in Table 4.

Table 4. Mass, energy, and exergy relations for the components of Brayton cycle.

Cycle components	Mass, energy, and exergy equations
 <p>Compressor I</p>	$\dot{m}_1 = \dot{m}_2$ $\eta_{compressor,I} = \frac{h_{2,s} - h_1}{h_2 - h_1}$ $\dot{W}_{compressor,I} = \dot{m}_{air}(h_2 - h_1)$ $(\psi_1 + \dot{W}_{compressor,I}) - \psi_2 - \dot{i}_{compressor,I} = 0$ $\eta_{II,compressor,I} = 1 - \left(\frac{\dot{i}_{compressor,I}}{\dot{W}_{compressor,I}} \right)$
 <p>Intercooler</p>	$\dot{m}_3 = \dot{m}_4$ $\dot{m}_{w3} = \dot{m}_{w4}$ $\dot{Q}_{intercooler} = \dot{m}_{w3}(h_{w4} - h_{w3})$ $\dot{Q}_{intercooler} = \dot{m}_{air}(h_3 - h_4)$ $(\psi_{w3} + \psi_3) - (\psi_{w4} + \psi_4) - \dot{i}_{intercooler} = 0$ $\eta_{II,intercooler} = 1 - \left(\frac{\dot{i}_{intercooler}}{\psi_3 - \psi_4} \right)$
 <p>Compressor II</p>	$\dot{m}_4 = \dot{m}_5$ $\eta_{compressor,II} = \frac{h_{5,s} - h_4}{h_5 - h_4}$ $\dot{W}_{compressor,II} = \dot{m}_{air}(h_5 - h_4)$ $(\psi_4 + \dot{W}_{compressor,II}) - \psi_5 - \dot{i}_{compressor,II} = 0$ $\eta_{II,compressor,II} = 1 - \left(\frac{\dot{i}_{compressor,II}}{\dot{W}_{compressor,II}} \right)$
 <p>Regenerator</p>	$\dot{m}_5 = \dot{m}_6 = \dot{m}_{10} = \dot{m}_{11}$ $\epsilon_{rej.} = \frac{T_{10} - T_{11}}{T_{10} - T_5}$ $\dot{Q}_{regenerator} = \dot{m}_{air}(h_5 - h_6)$ $\dot{Q}_{regenerator} = \dot{m}_{air}(h_{10} - h_{11})$ $(\psi_5 + \psi_{10}) - (\psi_6 + \psi_{11}) - \dot{i}_{regenerator} = 0$ $\eta_{II,regenerator} = 1 - \left[\frac{\dot{i}_{regenerator}}{(\psi_{10} - \psi_{11})} \right]$
 <p>Combustion Chamber</p>	$\dot{m}_6 = \dot{m}_7$ $\dot{Q}_{combustion\ chamber} = \dot{m}_{air}(h_7 - h_6)$ $\psi_6 + \left(1 - \frac{T_0}{T_7} \right) \dot{Q}_{comb.cham.} - \psi_7 - \dot{i}_{comb.cham.} = 0$ $\eta_{II,comb.cham.} = 1 - \frac{\dot{i}_{comb.cham.}}{\left(1 - \frac{T_0}{T_7} \right) \dot{Q}_{comb.cham.}}$
 <p>Turbine I</p>	$\dot{m}_7 = \dot{m}_8$ $\eta_{turbine,I} = \frac{h_7 - h_8}{h_7 - h_{8,s}}$ $\dot{W}_{turbine,I} = \dot{m}_{air}(h_7 - h_8)$ $\psi_7 - (\dot{W}_{turbine,I} + \psi_8) - \dot{i}_{turbine,I} = 0$ $\eta_{II,turbine,I} = 1 - \left[\frac{\dot{i}_{turbine,I}}{(\psi_7 - \psi_8)} \right]$
 <p>Reheater</p>	$\dot{m}_8 = \dot{m}_9$ $\dot{Q}_{reheater} = \dot{m}_{air}(h_9 - h_8)$ $\psi_8 + \left(1 - \frac{T_0}{T_9} \right) \dot{Q}_{reheater} - \psi_9 - \dot{i}_{reheater} = 0$ $\eta_{II,reheater} = 1 - \frac{\dot{i}_{reheater}}{\left(1 - \frac{T_0}{T_9} \right) \dot{Q}_{reheater}}$
 <p>Turbine II</p>	$\dot{m}_9 = \dot{m}_{10}$ $\eta_{turbine,II} = \frac{h_9 - h_{10}}{h_9 - h_{10,s}}$ $\dot{W}_{turbine,II} = \dot{m}_{air}(h_9 - h_{10})$ $\psi_9 - (\dot{W}_{turbine,II} + \psi_{10}) - \dot{i}_{turbine,II} = 0$ $\eta_{II,turbine,II} = 1 - \left[\frac{\dot{i}_{turbine,II}}{(\psi_9 - \psi_{10})} \right]$

The pressure at the first stage compressor by changing intercooling pressure ratio is found out in Eq. 3

$$r_{pi} = \frac{P_2}{P_1} \quad (3)$$

The net power output by the Brayton cycle is evaluated by using Eq. 4

$$\dot{W}_{net,brayton} = (\dot{W}_{turbine,I} + \dot{W}_{turbine,II}) - (\dot{W}_{compressor,I} + \dot{W}_{compressor,II}) \quad (4)$$

The thermal efficiency of Brayton cycle is defined in Eq. 5

$$\eta_{brayton} = \frac{\dot{W}_{net,brayton}}{\dot{Q}_{combustion\ chamber} + \dot{Q}_{reheater}} \quad (5)$$

The net power output by the combined cycle is obtained by solving Eq. 6

$$\dot{W}_{net,total} = \dot{W}_{net,ORC} + \dot{W}_{net,brayton} \quad (6)$$

The thermal efficiency of the combined organic Rankine-Brayton cycle is calculated by solving Eq. 7

$$\eta_{total} = \frac{\dot{W}_{net,total}}{\dot{Q}_{combustion\ chamber} + \dot{Q}_{reheater}} \quad (7)$$

Utilization efficiency of the combined cycle is given by Eq. 8

$$\eta_{utilization} = \frac{\dot{W}_{net,ORC}}{\dot{m}_{air}((h_{11}-h_{13})-T_0(s_{11}-s_{13})) + \dot{m}_{air}((h_2-h_3)-T_0(s_2-s_3))} \quad (8)$$

RESULTS AND DISCUSSIONS

Figure 4 gives variation of net power produced by ORC, Brayton and combined cycle with respect to gas turbine inlet temperature. Increasing turbine inlet temperatures lead to increase net power produced for all cycles. The reason of increasing of net power produced by Brayton cycle is that heat input to the cycle takes place at high temperature. When the gas turbine inlet temperature raises, turbine outlet temperature increases. Hence, heat source temperature of ORC increases as well. This situation increases net power produced. The pinch point temperature difference is constant at 12.5°C in Figure 4.

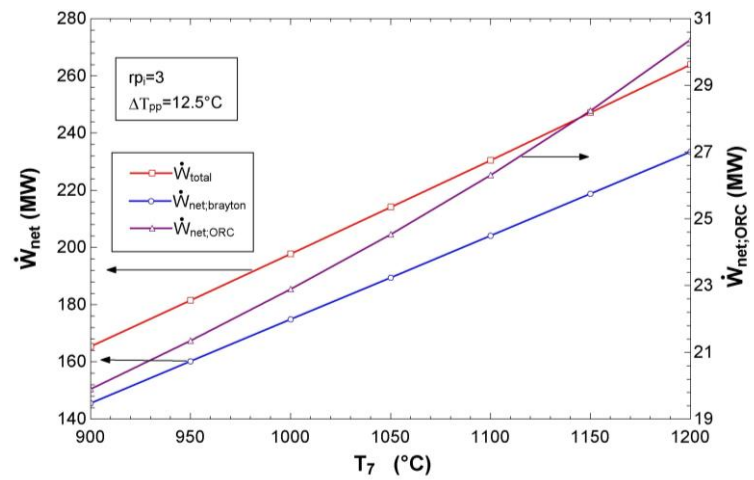


Figure 4. Effect of gas turbine inlet temperature on the net power produced by ORC, Brayton and combined cycle

The evaporator pressure increases due to the increased heat source temperatures because pinch point temperature difference is kept constant at 12.5°C. The mass flow rate of working fluid in ORC increases because the enthalpy difference at ascending evaporator pressure decreases. Owing to this parabolic increase, the increase in net power produced by ORC also shows a parabolic tendency. The net power produced by adding ORC to the Brayton cycle as a bottoming cycle is increased by an average of 11.6%.

Figure 5 demonstrates the difference in thermal efficiency of ORC, Brayton, and combined cycle under the same conditions. The thermal efficiency increasing of Brayton cycle is an expected result for increasing turbine inlet temperatures. The increase in thermal efficiency of ORC is also due to the increase in heat source temperature. While the turbine inlet temperature is 900 °C, the evaporator inlet temperature in Brayton cycle is 271.7 °C. On the other hand, when the turbine inlet temperature is 1,200 °C, the evaporator inlet temperature in Brayton cycle is 321.8 °C. In Figure 4, while the net power produced by ORC shows an increasing tendency, the thermal efficiency shows a decreasingly growing trend. This is due to the increase in heat input to ORC at increasing heat source temperature.

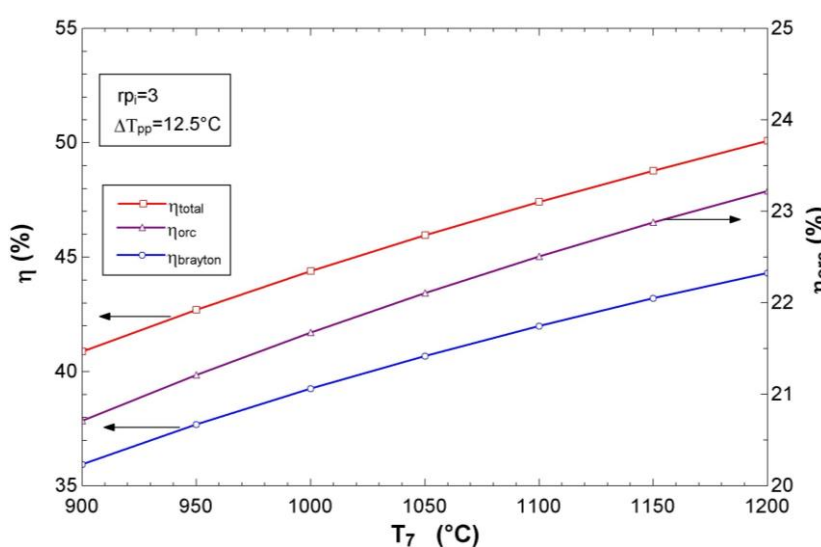


Figure 5. ORC and combined cycle efficiency as a function as of gas turbine inlet temperature

Figure 6 presents the variation of heat drawn by the preheaters, evaporator and net power produced by bottoming ORC via evaporator effectiveness. In order to increase efficiency of any power cycle, it is necessary to draw heat from relatively high temperature sources. In the present cycle, high temperature heat source is exit air of regenerator. Therefore, evaporator is the key equipment in terms of heat exchange process in the ORC. As effectiveness of the evaporator increases, the rate of heat removed from the heat source in it increases as well. Consequently, higher net power production can be obtained. Since pinch point temperature is T_{12} , higher heat removing cause to decrease the T_{12} . Thus, reduction in evaporator pressure occurs. Temperature differences in the evaporator between air and the working fluid get higher progressively, and it means lower exergy efficiency of the evaporator (Figure 15). Temperature difference of working fluid through the preheater additionally decreases due to lower evaporator pressure, and it determines the behavior of the preheater 2.

Figure 7 gives heat exchange process of heat exchangers in ORC. While the most heat exchange occurs in the evaporator, the least heat exchange process occurs in the preheater II.

The effect of different intercooling pressure ratio (r_{pi}) on the thermal efficiency of ORC and combined cycle can be seen in Figure 8. The thermal efficiency of ORC raises with increasing intercooling pressure ratio. The reason of this situation is that turbine outlet temperature increases at increasing intercooling pressure ratios. The hot air enters to the evaporator of ORC depending on intercooling pressure ratio. A method to increase the efficiency is also to increase heat source temperature in Rankine cycle. It can be inferred that increasing the differences of pinch point temperature would be the consequence of the reduction of the thermal efficiency of ORC. However, the highest thermal efficiency of the combined cycle is obtained in the lowest pinch point temperature difference. The thermal efficiency of combined cycle by adding ORC to Brayton cycle is increased by 11.7% depending on different intercooling pressure ratio.

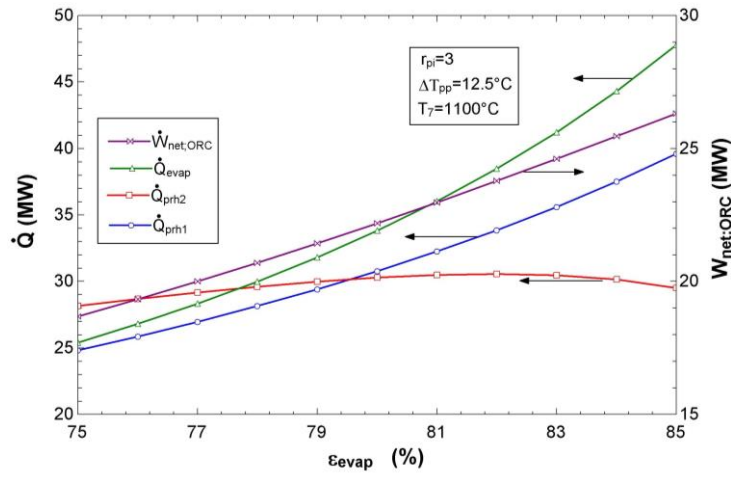


Figure 6. Net power produced by ORC and heat input to ORC versus evaporator effectiveness

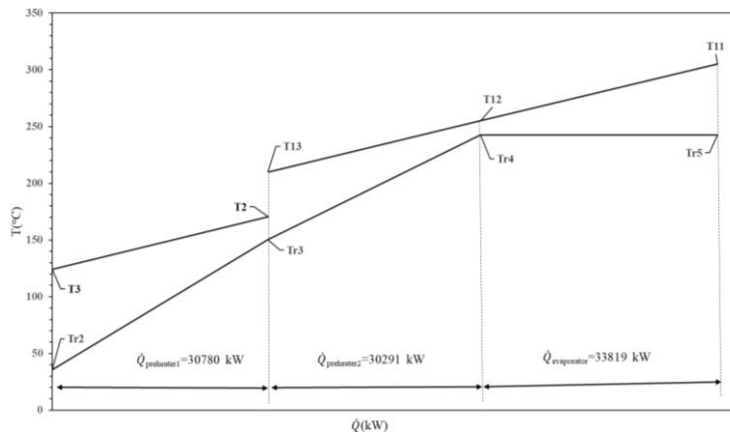


Figure 7. Heat exchange process of heat exchangers in ORC

The effect of intercooling pressure ratio and pinch point temperature difference on thermal and utilization efficiency of ORC is given in Figure 9. According to Figure 9 as the thermal efficiency of ORC increases at high inter cooling pressure ratios. Utilization efficiency initially increases with pressure ratio after that it shows descending tendency.

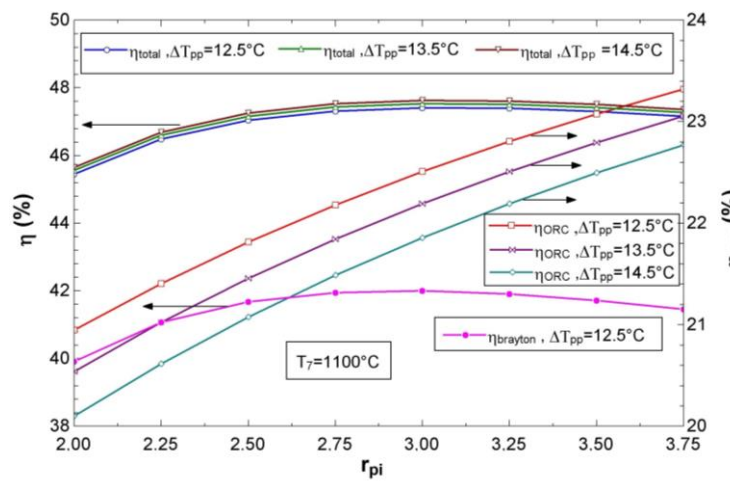


Figure 8. Effect of intercooling pressure ratio and pinch point temperature difference on thermal efficiency of ORC and combined cycle

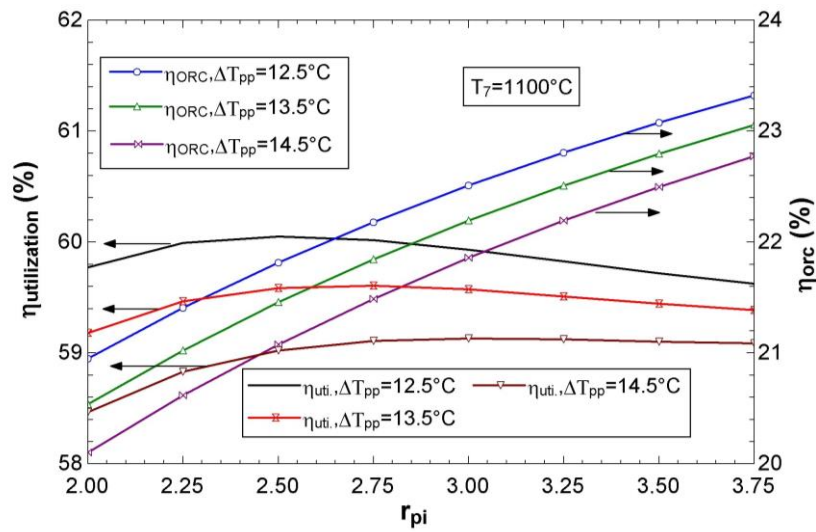


Figure 9. Effect of intercooling pressure ratio and pinch point temperature difference on thermal and utilization efficiency of ORC

The effect of different intercooling pressure ratio on the net power produced by ORC and combined cycle is presented in Figure 10. The net power produced increases with increasing intercooling pressure ratio. The net power produced by ORC increases at increasing pinch point temperature difference.

Figure 11 gives the variation of net power and thermal efficiency with evaporator effectiveness for different working fluids. In Figure 11 at ascending evaporator effectiveness, the net power produced by ORC increases. However, the thermal efficiency of ORC decreases because the rate of increase of heat input to the ORC is higher than the rate of increase of net work output in ORC. When the effectiveness of evaporator varies from 0.75 to 0.85, net work output in ORC and heat input to the ORC vary between 18.7-26.3 MW and between 78.4-116.9 MW, respectively.

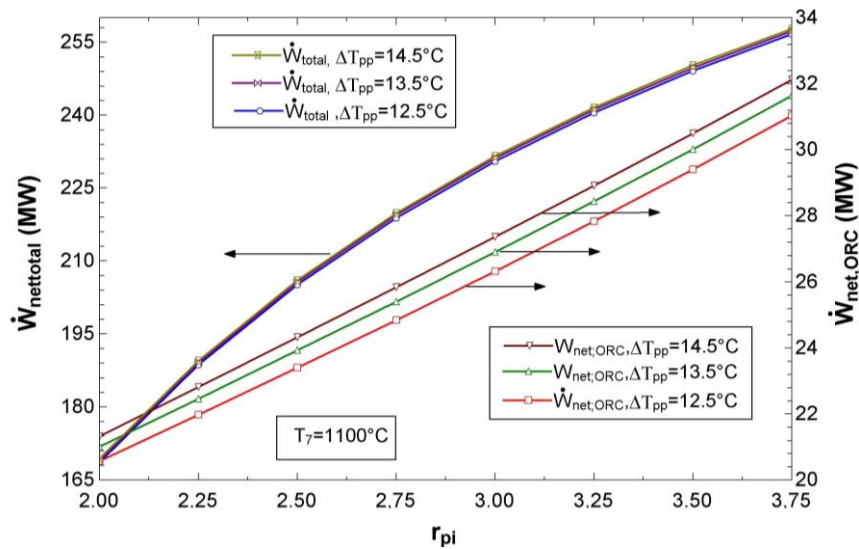


Figure 10. Effect of intercooling pressure ratio and pinch point temperature difference on the net power produced by ORC and combined cycle

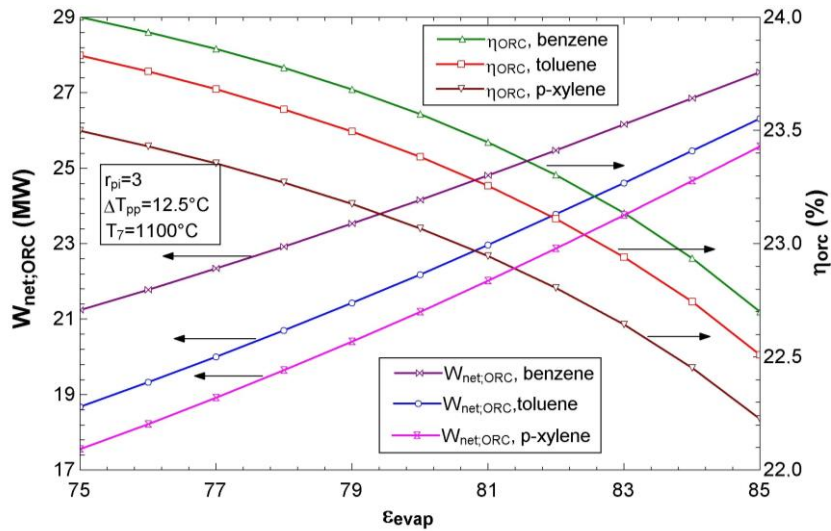


Figure 11. The variation of net power and thermal efficiency with evaporator effectiveness

Figure 12 reveals the variation of thermal efficiency and utilization efficiency with intercooling pressure ratio. The thermal efficiency of combined cycle increases at higher intercooling pressure ratio. Utilization efficiency initially increases but later it decreases because the rate of exergy input increase is more according to exergy output at higher intercooling pressure ratio. While the pressure ratio is 3, the maximum thermal efficiency of combined cycle is 47.4%. On the other hand, when the pressure ratio is 2.5, the maximum utilization efficiency is 60.05%.

Figure 13 represents the exergy losses in ORC. While the greatest exergy destruction takes place at the expander, the lowest exergy destruction occurs in the pump of the ORC. Exergy losses in the components; 54.19 kW in pump, 1,025 kW in preheater II, 2,524 kW in evaporator, 3,532 kW in condenser, 3,772 kW in preheater I, 5,329 kW in expander. As a percentage; 0.33% in pump, 6% in preheater II, 16% in evaporator, 22% in condenser, 23% in preheater I, 33% in expander.

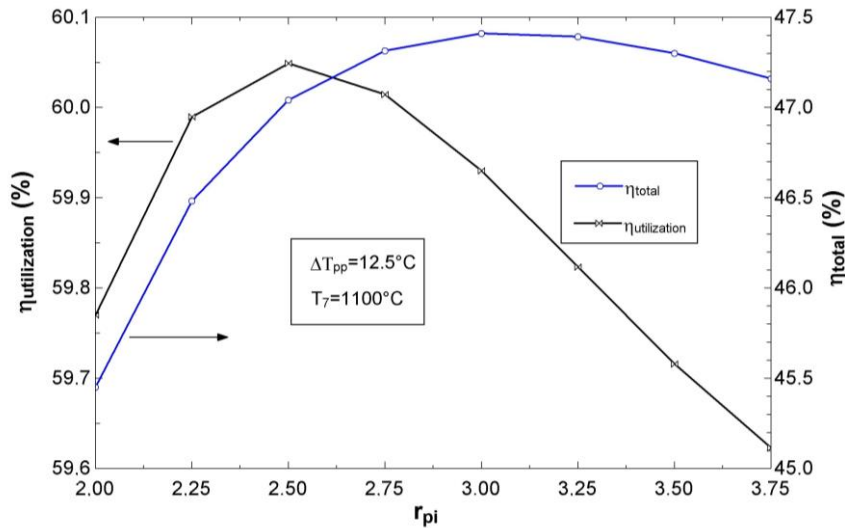


Figure 12. Variation of thermal efficiency and utilization efficiency with respect to intercooling pressure ratio

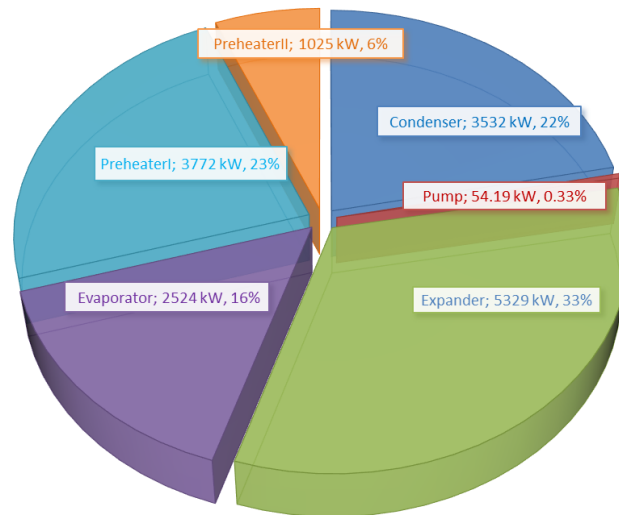


Figure 13. Exergy losses diagram

Figure 14 and 15 gives variation of components exergy efficiency according to intercooling pressure ratio and evaporator effectiveness, respectively. According to intercooling pressure ratio, the preheater 2 has the greatest exergy efficiency; on the other hand, with respect to evaporator effectiveness, the evaporator has greatest exergy efficiency. In both cases, the condenser has the lowest exergy efficiency in ORC.

CONCLUSIONS

The performance analysis of created combined cycle by adding ORC as a bottoming cycle for intercooling and reheating Brayton cycle has been performed in the present work. The thermal efficiency of combined cycle is higher about 11.7% than thermal efficiency of Brayton cycle. Moreover, the net power produced by ORC has contributed nearly 28,650 kW. In terms of second law, highest exergy loss occurs at total heat exchange (preheater I, II and evaporator) process from the waste heat as 7,321 kW and 45% of total exergy loss in ORC, whereas turbine has highest individual exergy loss of all as 5,329 kW and 33%. Another result of why ORC would be beneficial as bottoming cycle is that using waste heat would rather increase produced power of ORC than only increase efficiency of ORC system. Moreover, in order to achieve higher power output for ORC, it would be needed higher compressibility ratios. It is finally worth to note that evaporator is the essential component of the ORC system.

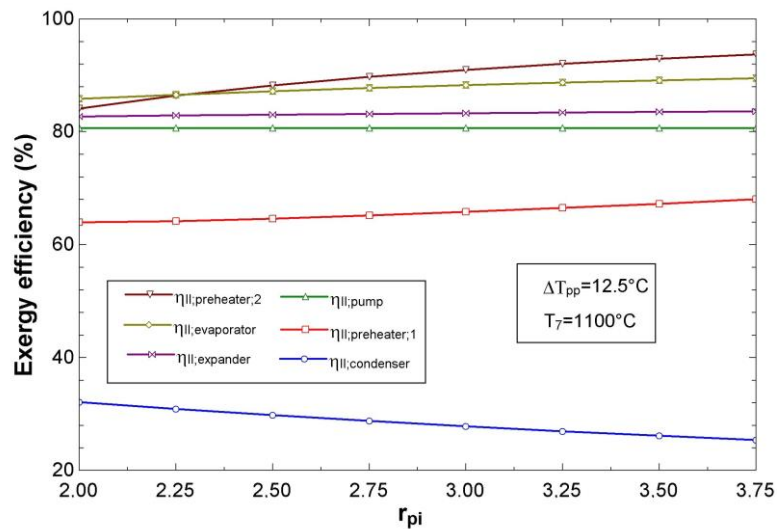


Figure 14. Variation of components exergy efficiencies with intercooling pressure

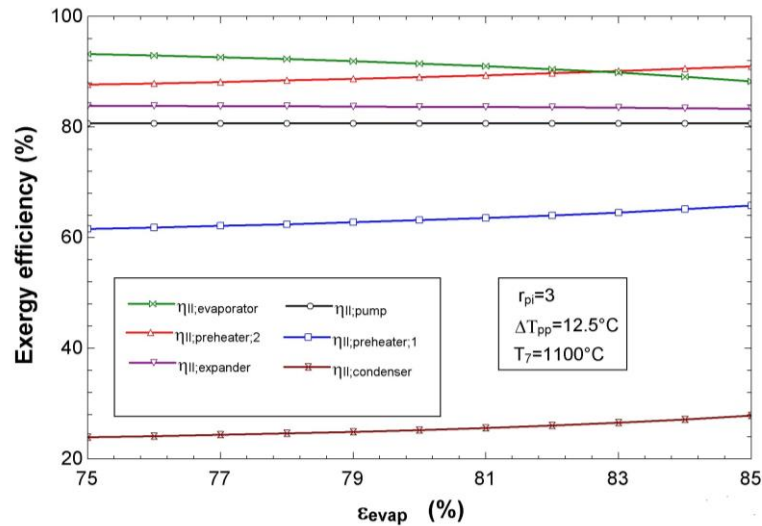


Figure 15. Variation of components exergy efficiencies with evaporator effectiveness

NOMENCLATURE

- h : Enthalpy (kJ/kg)
 \dot{i} : Exergy destruction (kW)
 P : Pressure (bar)
 \dot{Q} : Thermal duty (MW)
 T : Temperature (°C)
 \dot{W} : Power (MW)
 r_{pi} : Intercooling pressure ratio
 s : Entropy (kJ/kg-K)

Greek symbols

- ε : Effectiveness
 η : Efficiency
 ΔT_{pp} : Pinch point temperature difference (°C)
 ψ : Exergy flow (kW)

Subscripts

- ORC : Organic Rankine cycle
 r : refrigerant

REFERENCES

- [1] He C, Liu C, Gao H, Xie H, Li Y, Wu S, et al. The optimal evaporation temperature and working fluids for subcritical organic Rankine cycle. *Energy*. 2012;38(1):136-43.
- [2] Carcasci C, Ferraro R, Miliotti E. Thermodynamic analysis of an organic Rankine cycle for waste heat recovery from gas turbines. *Energy*. 2014;65:91-100.
- [3] Yari M, Mahmoudi S. Utilization of waste heat from GT-MHR for power generation in organic Rankine cycles. *Applied Thermal Engineering*. 2010;30(4):366-75.
- [4] Clemente S, Micheli D, Reini M, Taccani R. Bottoming organic Rankine cycle for a small scale gas turbine: A comparison of different solutions. *Applied energy*. 2013;106:355-64.
- [5] Roy J, Misra A. Parametric optimization and performance analysis of a regenerative Organic Rankine Cycle using R-123 for waste heat recovery. *Energy*. 2012;39(1):227-35.
- [6] Wang Z, Zhou N, Guo J, Wang X. Fluid selection and parametric optimization of organic Rankine cycle using low temperature waste heat. *Energy*. 2012;40(1):107-15.
- [7] Sun J, Li W. Operation optimization of an organic Rankine cycle (ORC) heat recovery power plant. *Applied Thermal Engineering*. 2011;31(11-12):2032-41.
- [8] Wei D, Lu X, Lu Z, Gu J. Performance analysis and optimization of organic Rankine cycle (ORC) for waste heat recovery. *Energy conversion and Management*. 2007;48(4):1113-9.
- [9] Ahmadi P, Dincer I, Rosen MA. Exergo-environmental analysis of an integrated organic Rankine cycle for trigeneration. *Energy Conversion and Management*. 2012;64:447-53.

- [10] Chacartegui R, Sánchez D, Muñoz J, Sánchez T. Alternative ORC bottoming cycles for combined cycle power plants. *Applied Energy*. 2009;86(10):2162-70.
- [11] Roy J, Mishra M, Misra A. Performance analysis of an Organic Rankine Cycle with superheating under different heat source temperature conditions. *Applied Energy*. 2011;88(9):2995-3004.
- [12] Liu B-T, Chien K-H, Wang C-C. Effect of working fluids on organic Rankine cycle for waste heat recovery. *Energy*. 2004;29(8):1207-17.
- [13] Meinel D, Wieland C, Spliethoff H. Effect and comparison of different working fluids on a two-stage organic rankine cycle (ORC) concept. *Applied Thermal Engineering*. 2014;63(1):246-53.
- [14] Cao Y, Gao Y, Zheng Y, Dai Y. Optimum design and thermodynamic analysis of a gas turbine and ORC combined cycle with recuperators. *Energy Conversion and Management*. 2016;116:32-41.
- [15] Eveloy V, Karunkeyoon W, Rodgers P, Al Alili A. Energy, exergy and economic analysis of an integrated solid oxide fuel cell–gas turbine–organic Rankine power generation system. *International Journal of Hydrogen Energy*. 2016;41(31):13843-58.
- [16] Kaşka Ö. Energy and exergy analysis of an organic Rankine for power generation from waste heat recovery in steel industry. *Energy Conversion and Management*. 2014;77:108-17.
- [17] Camporeale SM, Pantaleo AM, Ciliberti PD, Fortunato B. Cycle configuration analysis and techno-economic sensitivity of biomass externally fired gas turbine with bottoming ORC. *Energy conversion and management*. 2015;105:1239-50.
- [18] Maraver D, Royo J, Lemort V, Quoilin S. Systematic optimization of subcritical and transcritical organic Rankine cycles (ORCs) constrained by technical parameters in multiple applications. *Applied energy*. 2014;117:11-29.
- [19] Li Y-R, Wang J-N, Du M-T. Influence of coupled pinch point temperature difference and evaporation temperature on performance of organic Rankine cycle. *Energy*. 2012;42(1):503-9.
- [20] Tian H, Shu G, Wei H, Liang X, Liu L. Fluids and parameters optimization for the organic Rankine cycles (ORCs) used in exhaust heat recovery of Internal Combustion Engine (ICE). *Energy*. 2012;47(1):125-36.
- [21] Karellas S, Leontaritis A-D, Panousis G, Bellos E, Kakaras E. Energetic and exergetic analysis of waste heat recovery systems in the cement industry. *Energy*. 2013;58:147-56.
- [22] Hajabdollahi Z, Hajabdollahi F, Tehrani M, Hajabdollahi H. Thermo-economic environmental optimization of Organic Rankine Cycle for diesel waste heat recovery. *Energy*. 2013;63:142-51.
- [23] Astolfi M, Romano MC, Bombarda P, Macchi E. Binary ORC (Organic Rankine Cycles) power plants for the exploitation of medium–low temperature geothermal sources–Part B: Techno-economic optimization. *Energy*. 2014;66:435-46.
- [24] Guo C, Du X, Yang L, Yang Y. Performance analysis of organic Rankine cycle based on location of heat transfer pinch point in evaporator. *Applied Thermal Engineering*. 2014;62(1):176-86.
- [25] Tuo H. Energy and exergy-based working fluid selection for organic Rankine cycle recovering waste heat from high temperature solid oxide fuel cell and gas turbine hybrid systems. *International Journal of Energy Research*. 2013;37(14):1831-41.
- [26] Bademlioglu AH. Exergy analysis of the organic rankine cycle based on the pinch point temperature difference. *Journal of Thermal Engineering*. 2019;5(3):157-65.
- [27] Özdemir E. THERMODYNAMIC ANALYSIS OF BASIC AND REGENERATIVE ORGANIC RANKINE CYCLES USING DRY FLUIDS FROM WASTE HEAT RECOVERY. *Journal of Thermal Engineering*. 2018;4(5):2381-93.
- [28] Koroglu T. Advanced exergy analysis of an organic Rankine cycle waste heat recovery system of a marine power plant. *Journal of Thermal Engineering*. 2017;3(2):1136-48.
- [29] Kerme E, Orfi J. Exergy-based thermodynamic analysis of solar driven organic Rankine cycle. *Journal of Thermal Engineering*. 2015;1(5):192-202.
- [30] Klein SA. *Engineering Equation Solver (EES) for Microsoft Windows Operating System: Academic Professional Version*. F-Chart Software, Madison, WI. 2012.
- [31] Cengel Y, Boles MA. *Thermodynamics: An Engineering Approach 4th Edition in SI Units*. Singapore (SI): McGraw-Hill. 2002.
- [32] Wu C, Chen L, Sun F. Performance of a regenerative Brayton heat engine. *Energy*. 1996;21(2):71-6.
- [33] Kaushik S, Tyagi S, Singhal M. Parametric study of an irreversible regenerative Brayton cycle with isothermal heat addition. *Energy Conversion and Management*. 2003;44(12):2013-25.
- [34] Al-Sulaiman FA, Dincer I, Hamdullahpur F. Exergy modeling of a new solar driven trigeneration system. *Solar Energy*. 2011;85(9):2228-43.